Underwater Sound Pulse Generator
U.S.P.G.

by

Jayson D. Strayer

Submitted to the Department of Electrical Engineering and Computer Science

in Partial Fulfillment of the Requirements for the Degrees of

Bachelor of Science in Electrical Science and Engineering

and Master of Engineering in Electrical Engineering and Computer Science

at the Massachusetts Institute of Technology

May 26, 1996

Author .....
Department of Electrical Engineering and Computer Science
May 16, 1996

Certified by ..
.....
Gerald L. Wilson
Thesis Supervisor

Accepted by ....
.....
F. R. Morganthaler
Chairman, Department Committee on Graduate Theses

Underwater Sound Pulse Generator
U.S.P.G.

by
Jayson D. Strayer

Submitted to the
Department of Electrical Engineering and Computer Science

May 26, 1996

In Partial Fulfillment of the Requirements for the Degree of
Bachelor of Science in Electrical Science and Engineering
and Master of Engineering in Electrical Engineering and Computer Science

ABSTRACT

An underwater generator of sonic pulses was designed and constructed. The Sea Grant Consortium at the Massachusetts Institute of Technology plans to use the generator onboard an Odyssey class Autonomous Underwater Vehicle (AUV). The generator is part of a sonar system to obtain sub-bottom profiles.

The thesis details the specifications that a sound pulse generator must meet in order to be an effective sonar source in an AUV. A description of the design decisions follows the specifications. The final design is described in detail. The thesis concludes with a characterization of the generator's performance and an evaluation of the prototype with respect to the specifications. Modifications that may be necessary in future applications are included.

Thesis Supervisor: Gerald L. Wilson
Title: Vannevar Bush Professor

Contents

List of Figures

List of Tables

Acknowledgements

A prototype system was developed by a team of MIT Ocean Engineering students in the spring of 1994. The prototype was invaluable as a learning and testing platform. I am very grateful for the fine job that those students did. In particular, I would like to recognize Claudia Rodriguez's effort on the prototype. It was her success with the sparker that led to this thesis.

List of Abbreviations and Symbols

AUV	Autonomous Underwater Vehicle
HVPS	High Voltage Power Supply
IGBT	Insulated Gate Bipolar Transistor
MCT	MOS Controlled Thyristor
RLC circuit	Resistor, Inductor and Capacitor in series
SCR	Silicon Controlled Rectifier
USPG	Underwater Sound Pulse Generator

Summary

The following paper describes the design and construction of an underwater sonic source. The prototype purposefully meets the constraints of an Autonomous Underwater Vehicle (AUV). Electric discharge is the selected method of sound generation. Most of the effort has been directed at the design of the discharge circuit with particular emphasis placed on the incorporation of low weight and low volume components. Other aspects of design include controlling circuitry and physical structure of the spark gap.

A simple electric discharge circuit is shown in Figure 0-1.

The voltage supply charges the capacitor. When the control circuitry closes the switch, the voltage is applied across the electrodes, which are immersed in water. If sufficient energy is stored in the capacitor, the water between the electrodes will breakdown, producing a sonic pulse.

The Underwater Sound Pulse Generator (USPG) described in this document expands upon this simple circuit to produce an efficient system, uniquely adapted to underwater seismic exploration. The USPG has been created for testing on an Odyssey class AUV.

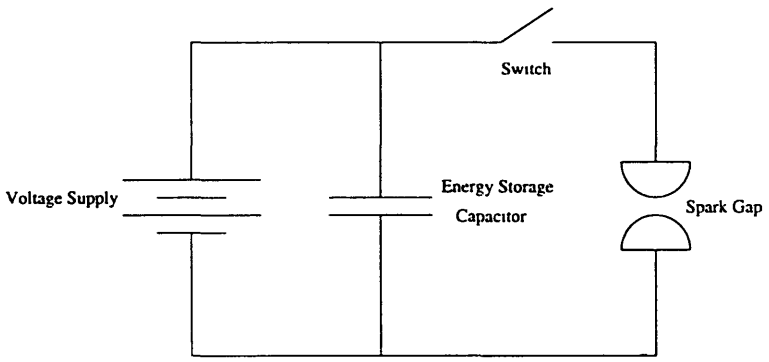

Figure 0-1: Basic Discharge Circuit

Chapter 1

Introduction

1.1 Motivation

Sub-bottom profiles of the ocean floor are useful to a wide variety of interests. Unfortunately, the methods for obtaining these profiles are expensive, cumbersome, and inefficient. An economical and autonomous profiling system is needed.

The applications of sub-bottom profiling range from industry to environment and from defense to entrepreneurship. In industry, the techniques can be used to locate features such as oil deposits or objects such as communication cables. Environmental seismic surveys map the amount and the movement of polluted sediment [13, 6]. The Navy is particularly interested in such a system for detecting mines. And the entrepreneur could use the technology to search for buried treasure or scare non-indigenous fish away from a hatchery.

A major challenge to the development of an efficient profiling system lies in the operating requirements of the sound pulse source. At the State University of Utrecht in The Netherlands, for example, both source and receiver have been developed for mapping industrial wastes. They are both mounted on a boat far-distant from the bottom to be profiled. Therefore, although the receiver and the recorder can run for hours on a 12V battery, the source needs a gasoline generator with support systems, including crew [6]. If the source can be made to fit on a small submarine such as an AUV, the AUV can descend near to the area to be profiled, record soundings, and

return, requiring much less energy in the sound source. One could further imagine a number of AUV's quickly profiling the bottom in a grid pattern. Thus, the creation of an efficient and autonomous source will eliminate many current constraints on profiling systems.

1.2 Objective

The purpose of this thesis is to construct a prototype underwater sound pulse generator for use on an AUV. A successful prototype will increase access to sub-bottom profiles in areas where such studies are now prohibitively expensive and cumbersome.

Many techniques produce sonic pulses, including explosives, air guns, water guns, and mechanical, magnetostrictive, piezoelectric, and eddy current transducers [2]. However, the sparker, or electric discharge system, is selected in part due to its simple design and lack of moving components. The thrust of the design effort, therefore, is to maximize the output of the discharge circuit while minimizing volume and mass.

Chapter 2

Specifications

Table 2.1 summarizes the specifications.

Parameter	Specification
Electrical Energy to Gap	20J
Battery Volume	3,400cm^3
Electronics Volume	6,360cm^3 in 18cm diameter, 25 cm length cylinder
Electrode Location	< 2m from electronics
Mass above displaced mass ($M - \rho_{water}V$)	5kg
Repetition Frequency	2 - 4 Hz
Energy Spectrum	< 10kHz
Lifetime	1,000 shots for 1 hour
Environment	fresh or salt water
Control	rising edge TTL

Table 2.1: Specifications Summary

The primary objective of this research was the creation of a 20 Joule (J) electrical pulse in water. Mounting in the AUV imposed the most severe constraints on achieving this objective. Other serious limitations on the design resulted from the desire for a rapid repetition rate and the optimization of the energy spectrum.

The specifications were formed by personnel at MIT's Sea Grant based on experience they had with the prototype developed by Claudia Rodriguez.

2.1 Acoustic Energy

The specification given was to increase the energy output of the prototype pulse by a factor of five. Therefore, the initial task was to determine the amount of energy in the prototype pulse. An estimate of 4J was obtained by integrating the product of the voltage across the gap and the current through the gap over time for one-half cycle.

$$E = \int_0^{\frac{T}{2}} i(t)v(t)dt$$

where E is the electrical energy into the gap, T is the period of the pulse, i(t) is the current through the spark gap, and v(t) is the voltage across the gap. Based on research by David Caulfield [2], the electrical energy is proportional to acoustic energy. Therefore, an $\int i(t)v(t)dt$ value of 20J across the spark gap became the specification.

The prototype was operated with a balloon shield surrounding the gap and it was later realized that the balloon was decreasing the acoustic output by as much as 50%. Since the USPG will operate without the balloon, an $\int i(t)v(t)dt$ energy of 10J may suffice. However, 20J was retained as the objective because of the unrepeatability of the prototype's pulse and the randomness of the balloon's effect.

2.2 Mounting in the AUV

The initial desire was to contain the entire assembly in an oil-compensated cylinder with dimensions 10cm diameter and 25cm length. However, after studying the type of equipment needed, the impracticality of this specification became evident. A capacitor and power supply would require at least that much volume. Additionally, the most practical power supply would be batteries that could not withstand a pressurized oil environment. After further reviewing the layout of the AUV, the following component distribution was agreed upon:

- Batteries housed in one of two uncompensated spheres with an available volume of 3,400cm^3

- Electronics located in an oil-compensated cylinder with dimensions of 18cm diameter and 25cm length
- Electrodes mounted outside the AUV, not more than 2m from the electronics

The wire interfaces and oil-compensated cylinder are provided by AUV specialists.

The mass of the system was to be less than 5kg more than the mass of the water displaced.

2.3 Repetition Rate

A discharge frequency of at least 2Hz, ideally 4Hz, was desired for 5cm resolution. From this information, it can be derived that the AUV can travel at a minimum speed between 0.72 km/hr and 0.36 km/hr as computed by

$$2Hz * 5cm = 10cm/s = 0.36km/hr$$

$$4Hz * 5cm = 20cm/s = 0.72km/hr$$

To obtain 20J in the pulse, the system needs 400W, assuming the same efficiency as the prototype, i.e. 20%.

$$20J * 4Hz * \frac{1}{0.20} = 400W$$

2.4 Energy Spectrum

Frequency content above 10 kHz was to be small. Therefore, the 20J goal for acoustic energy needs to be computed in the frequency spectrum by summing the energy in the 0 Hz to 10 kHz regime as follows

$$\sum_{f=0Hz}^{10kHz} E(f)$$

2.5 Lifetime

The design was to provide for 1 hour of continuous duty at 4Hz. This specification implies that the batteries will need to supply approximately 1MJ and that the electrodes cannot deteriorate significantly over 14,400 shots.

In actuality, the AUV will fire at a reduced repetition rate until something interesting is found. Then it will fire at the maximum rate. Therefore, the system should consume less energy and fire less shots during this searching phase. The final specification was for 1,000 shots over the course of one hour.

2.6 Environment

Operation at pressures up to 10,000psi was desired. However, in practice, the AUV will initially be operated in shallow waters. The effect of greater depths will be tested in the field later. The design effort, therefore, was allowed to focus on the other specifications. The components were selected with assurances from the manufacturer that operation in oil was acceptable. However, most manufacturers could provide no information on the effects of high pressure on their products. In addition, research by Jones and Kunhardt [8] indicates that the spark is dependent upon pressure.

The system was to function in the Charles River and in salt water.

2.7 Control

Discharge should occur after receiving the rising edge of a TTL signal from AUV electronics.

Chapter 3

Design

A system for creating electronic discharges naturally breaks down into four subsystems:

1. Disharge Circuit
2. Control Circuit
3. Spark Gap
4. Power Source

The discharge circuit controls the frequency and the energy of the acoustic pulse. The control circuit processes signals from the AUV electronics to open and close the switch of Figure 0-1. The acoustic pulse forms at the spark gap. The power source supplies energy forms the control and discharge circuits can use.

Geographically, the discharge circuit and control circuit are housed in an oil-compensated cylinder and the spark gap fires in the water. The power source consists of batteries and DC-DC converters, which convert battery voltage into usable voltage levels. The batteries reside in an uncompensated sphere or their own separate housing. The DC-DC converters are with the discharge and control circuits in the oil-compensated cylinder. The general scheme can be seen in Figure 3-1.

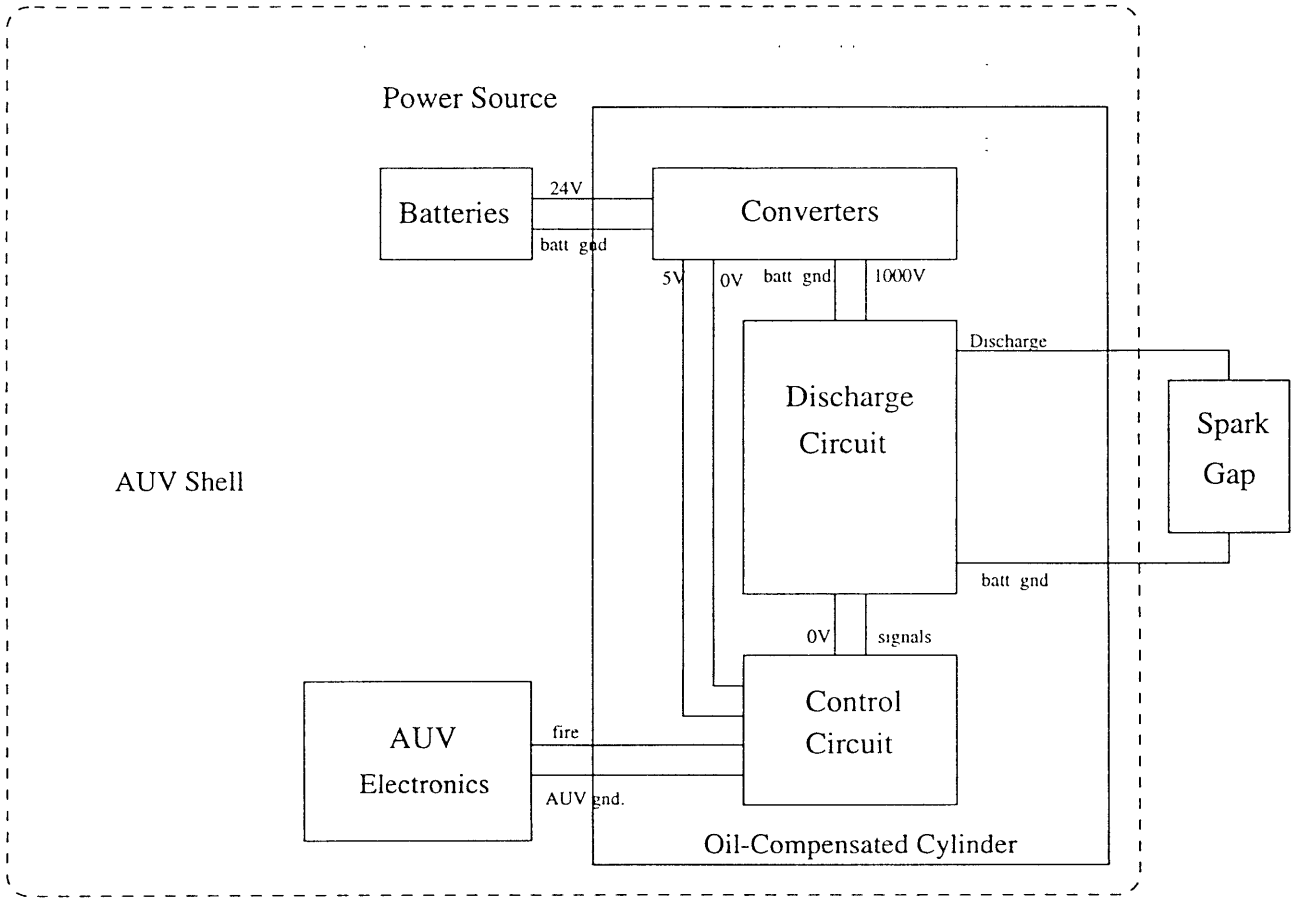

Figure 3-1: USPG Configuration

3.1 Discharge Circuit

The discharge circuit determines the qualities of the breakdown at the electrodes. The qualities to be controlled are energy and frequency. A simple RLC circuit can control current and frequency. Since the energy is approximately proportional to the square of the current, $\int i^2(t)Rdt$, the discharge circuit need only be slightly more complicated than an RLC circuit.

3.1.1 RLC Circuit Analysis

For an RLC circuit, such as in Figure 3-2, with initial conditions $v_C(t=0) = V_0$ and $i_L(t=0) = 0$

$$i_L(t) = \frac{V_0}{L\omega} e^{-kt} sin(\omega t)$$

where

$$k = \frac{R}{2L}$$

$$\omega = \sqrt{\frac{1}{LC} - k^2}$$

Thus, the current, $i_L(t)$, and the frequency, $f = \frac{\omega}{2\pi}$, can be controlled by varying the parameters L and C.

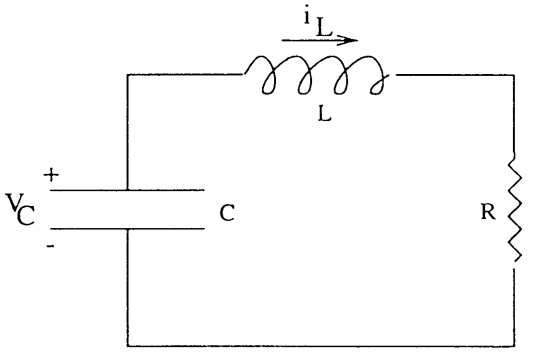

Figure 3-2: RLC Circuit

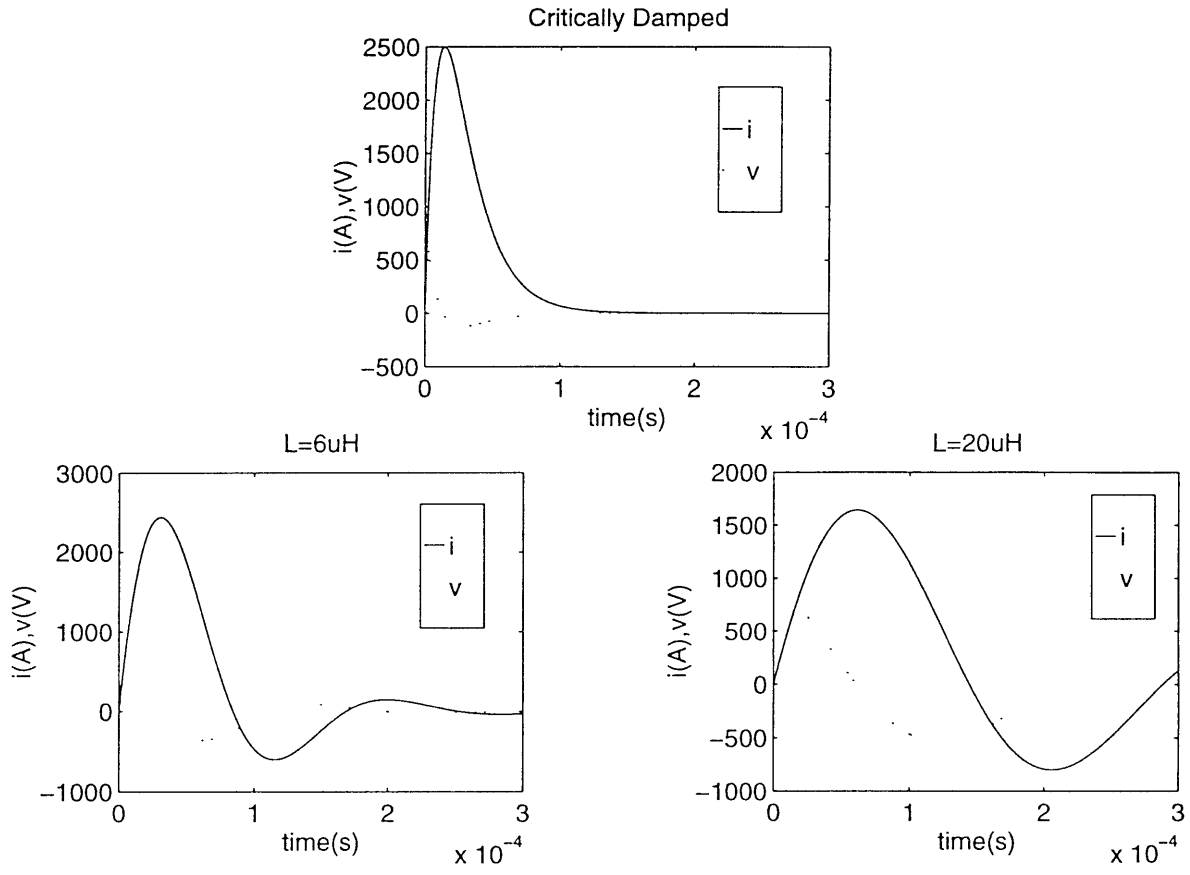

Figure 3-3: Possible $v_C(t)$ and $i_L(t)$

3.1.2 Circuit Layout

The specifications cause the designer to be interested in two waveforms of an RLC circuit — $v_C(t)$ and $i_L(t)$. The importance of $i_L(t)$ to energy into the gap has just been discussed. The value of $v_C(t)$ lies in the repetition rate. Consider the waveforms of Figure 3-3.

The critically damped waveform at the top would deposit all of the energy in the capacitor into the gap. At first glance, this is the best waveform. To see if it is viable, consider the practical values. Available devices limit $v_C(t = 0)$ to 1 kV. Since the prototype was only 20% efficient and the specifications call for 20J into the gap,

$$\frac{1}{2}CV^2 = 20J * \frac{1}{0.20} = 100J$$

The resulting implication is that C=200μF. Because the designed system is more efficient, C = 100μF is acceptable. The capacitance C should be as small as possible to meet the specifications of volume, mass, and repetition rate (minimizing the RC time constant for charging). For critical damping,

$$\omega = \sqrt{\frac{1}{LC} - k^2} = 0$$

$$\frac{1}{LC} = k^2 = \frac{R^2}{4L^2}$$

$$R = 2\sqrt{\frac{L}{C}} = 200\sqrt{L}$$

The inherent inductance of the discharge circuit will be around 2μH, meaning $R = 0.3\Omega$. Since the equivalent resistance across the spark is around 0.1Ω, the maximum efficiency would be $0.1/0.3 = 33\%$. The primary frequency component under these circumstances is greater than the 10 kHz desired and changes will decrease the efficiency. Thus the critically damped circuit is not a desirable choice.

The waveforms in the lower left and right of Figure 3-3 display the impact of changing L in an RLC circuit with R=0.2Ω and C=100μF. There are two important points to make here. First, the only current of value to the spark gap is in the first half cycle. After the first half-cycle has passed, the arc in the spark gap extinguishes. Any further appreciable current through the spark gap will need to reinitiate the arc, creating another sonic pulse. This is highly undesirable for seismic profiling. Second, adding inductance decreases frequency and peak current. Of course, adding capacitance increases peak current while decreasing frequency, but, as previously stated, the lower the capacitance, the better.

Fortunately the situation can be improved by adding a diode as in Figure 3-4. Now, the capacitor can discharge in the first half cycle of the current waveform. But, rather than being cut-off, the current flows through the diode to put some of the charge back onto the capacitor. The more efficient this secondary RLC circuit is, the higher the voltage left on the capacitor will be and the higher the possible repetition

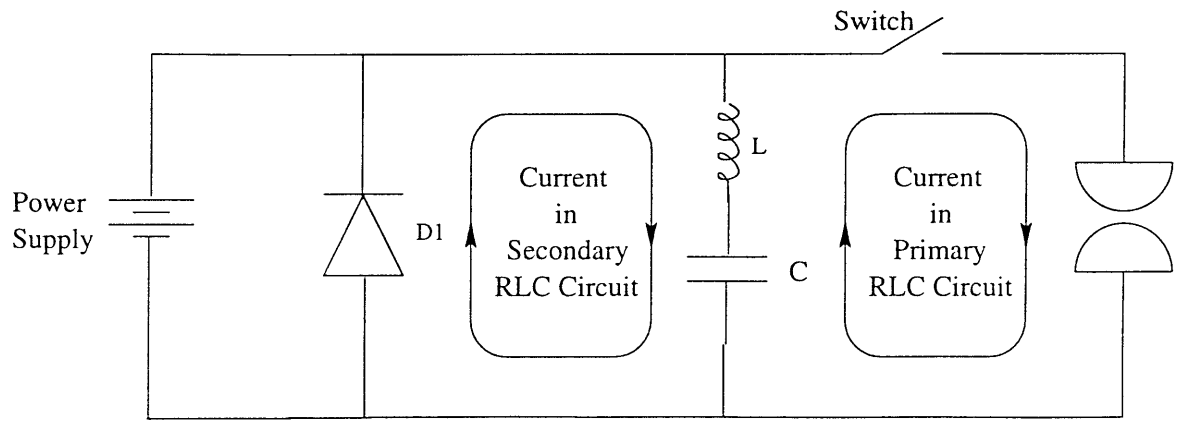

Figure 3-4: Optimized Discharge Circuit

rate. Clearly, the inherent inductance and resistance should be small to increase efficiency.

One might think that L and C can now be freely selected to match frequency and energy specifications. However, there are further considerations, such as the current capacity and switching time of the switch, the current capacity and switching time of the diode, and the current and reverse voltage ratings of the capacitor.

3.1.3 Component Selection

Three components must be bought for the USPG discharge circuit: capacitor, diode, and switch.

Capacitor

The selected capacitor is more robust than necessary. It is rated for 2 kV, so some mass and volume could be saved here. However, the effect of reverse voltage on the expected life of the capacitor should be considered before this capacitor is replaced. Likewise, capacitors have maximum repetition frequency and maximum current limits. For the selected capacitor, the current rating is 2kA and the repetition rate is 2 Hz. But, because of the excess in voltage rating, the capacitor can operate at 4Hz without ill effect. These concerns need to be directed to the manufacturer. Refer to

page 50 for more information on changing the capacitor.

Diode

The diode should have three characteristics. First, it needs to block greater than 1 kV. Second it needs to conduct 1,000 A in a pulse. Third it needs to turn on and off quickly. The efficiency of the secondary RLC circuit will suffer as these turn-on and turn-off times increase. A large turn-on time can also damage the power supply by not protecting it from large current and voltage pulses.

Switch

The most fundamental part of the design of the USPG is the selection of the switch. Clearly, the following attributes are necessary:

Fast turn-on Any conduction before breakdown will be energy lost. All the voltage needs to be applied at once.

2,000 A peak pulsed current rating

Greater than 1,000 V rating

Low on-state power dissipation

Turn-Off characteristics The switch needs to open when the current through the spark gap reaches some small threshold value.

Fast current rise $\frac{di}{dt} > 50A/\mu s$

The primary impact of the switch selection was the operating voltage. In some cases, a voltage greater than 1 kV may be appropriate (see page 50). However, switching large voltages requires large, puck devices that need an additional clamp so that current is evenly distributed throughout the semiconductor. After investigating the mass and volume associated with these puck devices, the superiority of operating in a voltage regime that could be handled by small devices became clear.

The most appropriate device for this application is the MOS-controlled thyristor (MCT). In addition to having a low on-state resistance, the MCT can be turned off by application of a reverse bias. Since the power supply is never turned off, this feature is attractive.

Unfortunately, the MCT is a new product of questionable reliability. In fact, there are none available until July 17,1996. Therefore, an alternative scheme using a typical phase-control silicon-controlled rectifier (SCR) was implemented. The voltage rating of the SCR is only 800 V and the peak pulsed current rating is only 550A. Although the voltage rating was not circumvented, the current and on-state power dissipation limits were overcome by paralleling four devices.

Furthermore, the SCR cannot be turned off at the gate, as is possible with the MCT. The SCR turns off when current falls below a threshold value, 75mA. The output current of the power supply (125mA each) is above threshold. Therefore, a scheme must be implemented to turn off the SCR. One scheme is to apply a negative bias to the gate, thereby increasing the threshold current. Another scheme is to add inductance to the secondary RLC circuit. An inductor added in series with the diode of Figure 3-4 will increase the impedance in the secondary RLC circuit, thereby creating a reverse voltage across the spark gap and the switch after the diode begins to conduct. This reverse voltage works against the power supply to turn off the SCR.

Other devices, such as IGBT's, could be used in a manner similar to an MCT. However, these devices dissipate significantly more power than an MCT [7].

3.2 Control Circuit

The control circuit receives a signal from the AUV electronics and opens or closes the switch based on that signal. A design based on an MCT and a deign based on an SCR were created.

The two designs share some principles. The AUV electronics need to be protected, so the signal is optically coupled to the control circuitry of the USPG. Both designs also use monostable vibrators to achieve the proper timing.

3.2.1 MCT

The MCT gate requires between +18V and +20V to turn the device off and between -7V and -20V to turn on. These voltages are referenced to the anode, the high voltage side of the switch. The current requirements of the gate call for greater than 1A. Because of the severity of these gate characteristics, the MCT requires a driver, the HIP20330. The HIP2030 can be purchased on its own evaluation board with optical isolation and other supporting components included. The package is called the HIP2030EVAL.

The primary challenge in the design of the TTL interface circuit is to account for different prebreakdown times. Prebreakdown is the period after the switch is closed, but before breakdown begins. If the MCT is turned off before breakdown begins, a spark will not form and the USPG will not generate sonic pulses. If the MCT is left on after the current pulse, the capacitor will discharge through the water. Since the length of prebreakdown varies, some form of feedback is necessary. Since this feedback should not add resistance to the discharge circuit, a Rigowski coil was chosen. See Section 4.2.1 for actual implementation.

3.2.2 SCR

The control circuit for an SCR is much simpler than for an MCT. First, the gate characteristics are reduced (1.5V trigger voltage, 50 mA trigger current). Second, the SCR is not turned off by the gate, so the feedback system is not needed.

3.3 Spark Gap

Four goals are reflected in the design of the spark gap: low prebreakdown loss, efficiency, large acoustic output, and long lifetime.

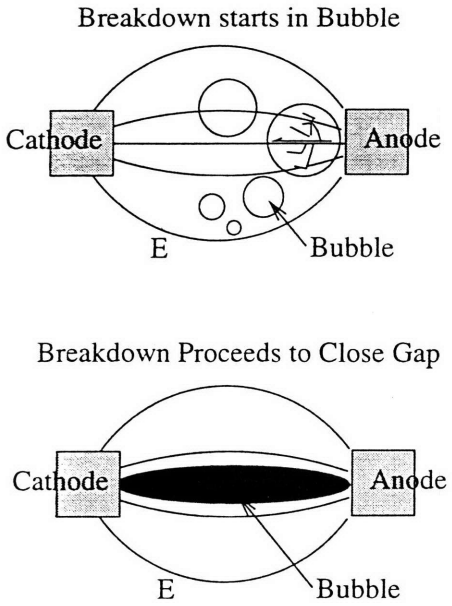

Figure 3-5: Possible Breakdown in Water

3.3.1 Low Prebreakdown Loss

Before breakdown the spark gap enters a period of conduction during which the capacitor is discharged with an RC time constant. A good design maximizes R while eliciting breakdown in a very short time.

At this point, a description of the breakdown process is in order. Breakdown is the result of an electric field. In a weakly ionized gas, the electric field accelerates electrons toward the anode. When the kinetic energy of the electron is greater than the energy required to free an electron from a neutral atom, an avalanche effect occurs. The result is a plasma that greatly reduces the resistance between the electrodes. The value of the electric field at which the avalanche occurs is called the breakdown electric field. In water, the breakdown process is not nearly so well understood. There is argument over whether the primary actions are electrical, thermal, or ionic [14]. However, it is known that after breakdown has begun, the heat of the discharge vaporizes the water, creating an expanding steam bubble. The expansion creates a shock wave – a sonic pulse. [4].

To minimize prebreakdown loss, it must be known what initiates breakdown so that the conduction period can be made small. According to Jones and Kunhardt,

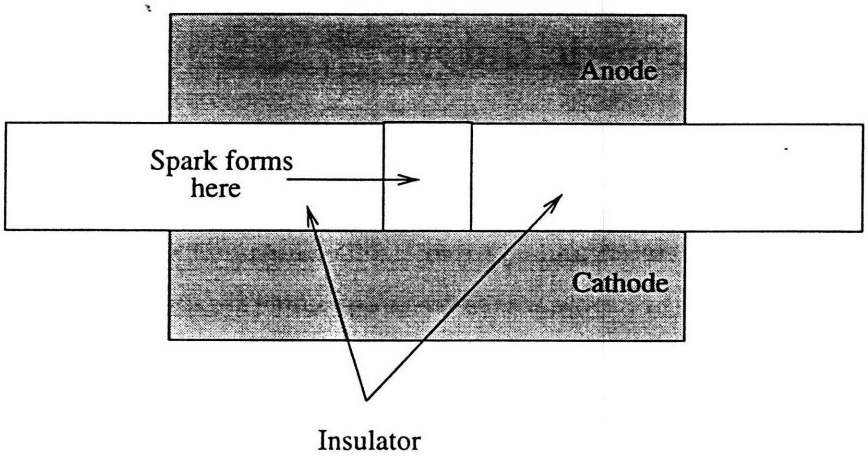

Figure 3-6: Ideal Spark Gap

breakdown cannot occur without bubble formation. In their view, the breakdown begins inside a bubble in a manner similar to the weakly ionized gas (see Figure 3-5). Therefore, to shorten the conduction period, bubbles should be formed quickly at locations of high electric field.

Electrolysis is one method of forming bubbles. A large current density, then, should quickly create bubbles in which breakdown can occur. Based on Ohm's Law,

$$\mathbf{J} = \sigma \mathbf{E}$$

the current density increases with electric field. If the current is too large, though, the capacitor will have discharged too much and the remaining voltage will not be high enough to produce the breakdown electric field. Since current is proportional to area by

$$I = \int_S \mathbf{J} \cdot \mathbf{dA}$$

the design should concentrate electric field through a small conducting area.

An ideal spark gap would be one such as is depicted in Figure 3-6. The area is confined so that there is no current in a region where the electric field and the current density cannot cause breakdown. Acoustic output and lifetime, however, do not allow

such designs.

3.3.2 Large Acoustic Output

The sonic pulse must be allowed to propagate freely out of the electrode region. For example, the balloon in Sea Grant's prototype decreased acoustic output by as much as 50% because it restricted pulse propagation. This means that the spark gap cannot be enclosed in insulation. Some stray current will therefore exist that will increase prebreakdown losses.

3.3.3 Long Lifetime

To attain a long electrode life there are two stategies that can be employed. First, the electrodes can be made out of a hard material. Experimental results indicate that the best material for spark gaps is $W + La_2O_3$ [5, 9]. Second, the surfaces of the anode and the cathode can be large so that the relative impact of each arc is reduced. This second strategy, however, must be weighed against the increase in prebreakdown loss that will accompany a larger conduction area.

3.3.4 Efficiency

If the equivalent circuit resistance of the electrodes during breakdown is large, then the $\int i^2(t) R_G dt$ at the gap is a greater percentage of the energy that was originally stored in the capacitor. So the chief concern in converting from stored electrical to acoustic energy is maximizing R_G, the resistance of the gap after breakdown, since i(t) is essentially a current source.

There are many ways to think about this conversion. Some attribute output acoustic energy to the volume of the arc's tree structure prior to breakdown [2, 11]. I doubt the accuracy of this explanation because the acoustic pressure is proportional to the current. A long current pulse in time corresponds to a long acoustic pulse in time. If the tree structure determined acoustic output, then the acoustic pulse should be fully formed prior to breakdown since the tree structure disappears once a

conduction path is formed. The duration of the acoustic pulse would be independent of the width of the current pulse.

The other method uses the volume and temperature of a current arc in air [3] to thermodynamically predict the pressure pulse in water. This method was not explored. The efficiency may be increased in the future by a better understanding of this method.

3.4 Power Source

Three primary devices compose the power source of the USPG. They are the batteries, the high voltage power supply (HVPS), and the 1kV isolation DC-DC converters.

Batteries

The batteries were not implemented during this research due to cost and availability. Instead, a Harrison Laboratories Model 520A regulated power supply was used. However, the batteries will need to provide 16A at 24V for 1 hour. The Yardney HR15 series meets these specifications.

HVPS

The batteries supply each Ultravolt 1C24-P125 unit with 24V. These HVPS's produce between 0V and 1,075V (electronically controlled) at 125mA. Two HVPS's connected in parallel are needed to guarantee a firing frequency that meets the specifications of 2-4Hz. These specific HVPS's were selected because of their high power density and shape. Although a single 250W unit is available that would eliminate the complexity of parallel operation, its length is unsuited for the cylindrical container described in the specifications.

Other Converters

Other voltage levels are necessary to power the control circuit and to drive the gate of the switch. In both the MCT and the SCR control circuits, these converters need to provide 1kV isolation between the gate and the batteries. If the isolation was not present, the voltage ratings of the AUV connectors would be violated. Both circuits require 5V to power the TTL circuitry. The SCR gate can be driven on the same converter. However, the MCT requires an additional 30V converter.

Chapter 4

Description

4.1 Discharge Circuit

A diagram of the discharge circuit appears in Figure 4-1. Table 4.1 describes the components. This section first simplifies the circuit and then analyzes the behavior of the circuit during a discharge.

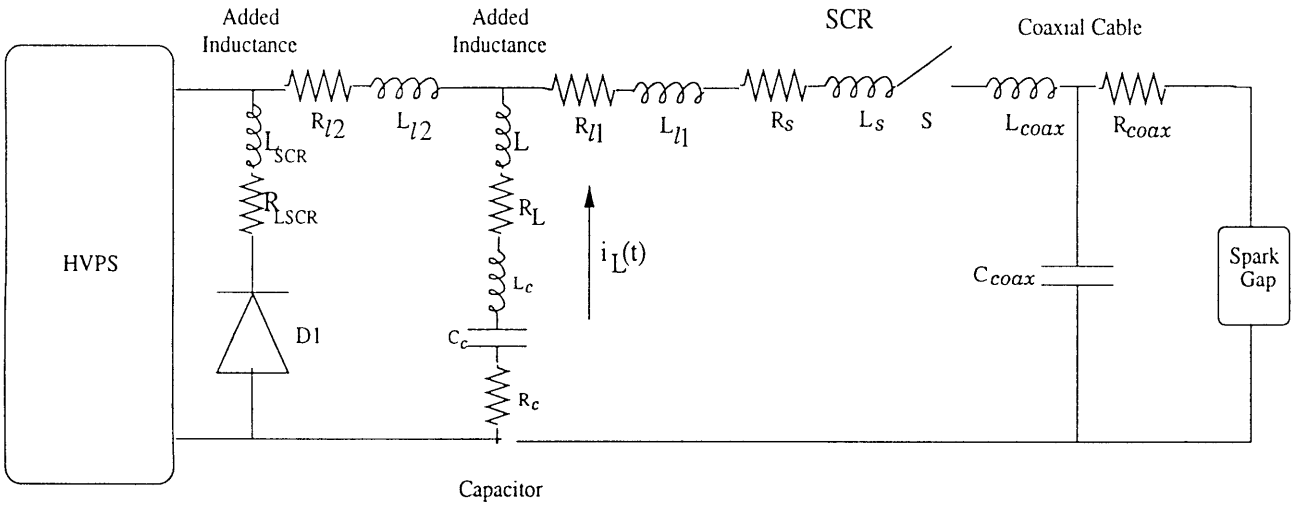

Figure 4-1: USPG Discharge Circuit

The first simplification to be made is the elimination of C_{coax}. The phase velocity of the coaxial cable is greater than $10^8 m/s$. Since the cable is only 2m long and

Component	Description	Value
$D1$	Diode	Harris RHRU100120
R_{l1}	Inherent Resistance of primary RLC circuit	0.01 Ω
L_{l1}	Inherent Inductance of primary RLC circuit	0.04 μH
R_{l2}	Inherent Resistance of secondary RLC circuit	0.01 Ω
L_{l2}	Inherent Inductance of secondary RLC circuit	0.2 μH
L_{SCR}	Secondary Added Inductance	1.8 μH
R_{LSCR}	Resistance of Added Secondary Inductor	0.03 Ω
L	Primary Added Inductance	11.4 μH
R_L	Resistance of Added Primary Inductor	0.04 Ω
Capacitor	Aerovox YD202EW110R	
L_C	Internal Inductance	1.5 μH
C_C	Capacitance	110 μF
R_C	Internal Resistance	0.086 Ω
SCR	Motorola MCR265-10 (4 in parallel)	
R_S	Equivalent Resistance	0.005 Ω
L_S	Equivalent Inductance	0.01 μH
S	Ideal Switch	
Coaxial Cable	RG8	
L_{coax}	Coaxial Cable (2m) Inductance	0.64 μH
R_{coax}	Coaxial Cable (2m) Resistance	0.01 Ω
C_{coax}	Coaxial Cable (2m) Capacitance	0.18 nF

Table 4.1: Discharge Circuit Component Description

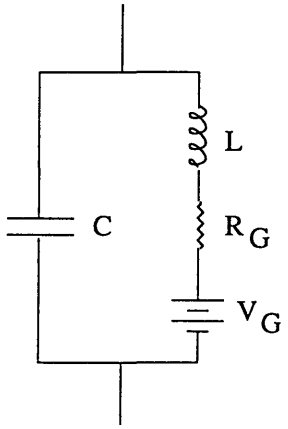

Figure 4-2: Spark Gap Circuit Model

the highest frequency component of interest is 10kHz, the voltage/current ratio of interest along the cable is nearly constant. At a voltage of 1kV, the cable capacitance could store $\frac{1}{2}CV^2 < 10^{-4}J$. Relative to the 50J stored in the primary capacitor, this energy will have minimal impact on the behavior of the circuit. Therefore, C_{coax} will be ignored.

The second simplification is a circuit description of the spark gap. The first model for the spark gap is shown in Figure 4-2. However, calculation reveals that the physical arrangement used leads to a capacitance of less than 10^{-4}nF. Since the capacitance of 0.18nF was ignored in the coaxial cable, this capacitance can be ignored as well. An inductance of 0.04μH was also calculated. This inductive element does not affect the transfer of energy from electric to acoustic, so it can be incorporated into L_{l1} of the simplified discharge circuit model (See Figure 4-3). The voltage source, V_G corresponds to a bonding energy that must be overcome during breakdown. Experimentally, the voltage was found to be roughly 30V. It always opposes the current through the gap. The resistance, R_G, was found to be 0.08Ω. It is the $\int i^2 R_G dt$ across this resistance that is converted to acoustic energy. The resulting simplified circuit is shown in

Figure 4-3 with values in Table 4.2. A comparison of $i_L(t)$ in this simplified circuit

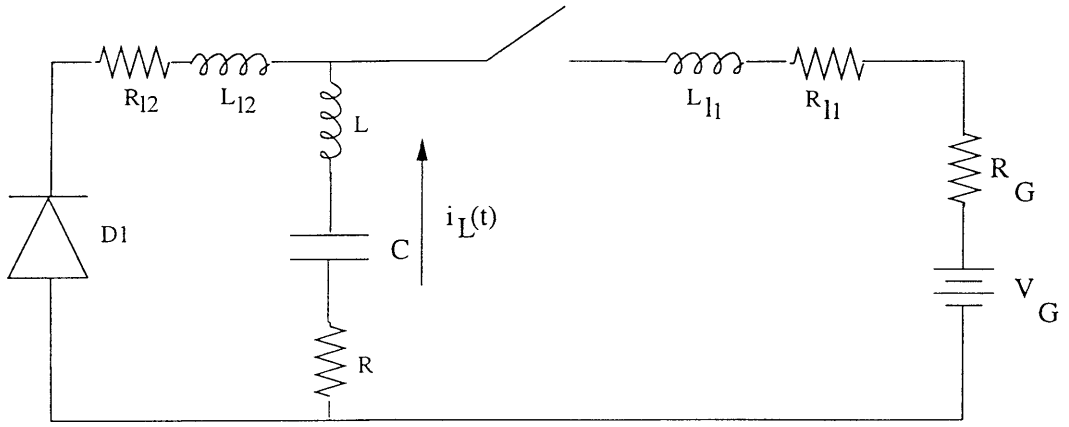

Figure 4-3: USPG Simplified Discharge Circuit

Component	Description	Value
$D1$	Diode	ideal
R_{L1}	Resistance of primary RLC circuit	0.025 Ω
L_{L1}	Inductance of primary RLC circuit	0.69 μH
R_{L2}	Resistance of secondary RLC circuit	0.04 Ω
L_{L2}	Inductance of secondary RLC circuit	2 μH
L	Inductance	12.9 μH
C	Capacitance	110μF
R	Resistance	0.13 Ω
S	Switch	ideal
R_G	Gap resistance	0.08 Ω
V_G	Voltage Source	30V

Table 4.2: Simplified Discharge Circuit Components

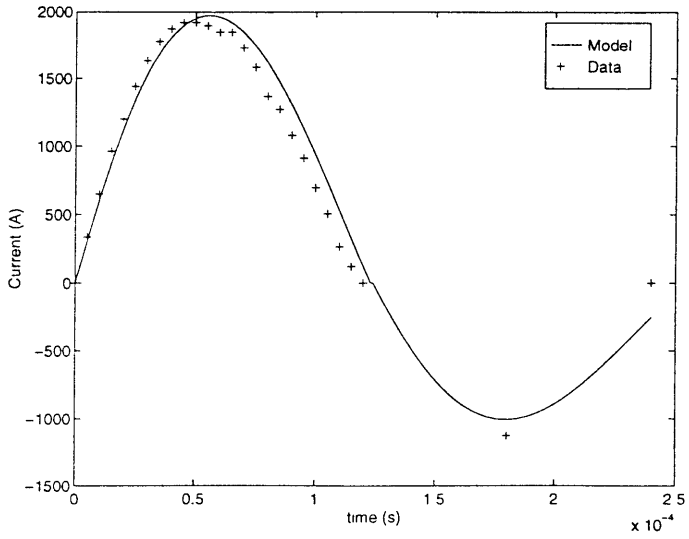

Figure 4-4: Model vs. Data

with data from the final prototype can be seen in Figure 4-4.

Prior to breakdown, the spark gap can be modelled as a simple resistor of value 300Ω.

Now that the circuit model is established, a description of the behavior of the circuit during a typical discharge is in order. References are made with respect to Figure 4-5.

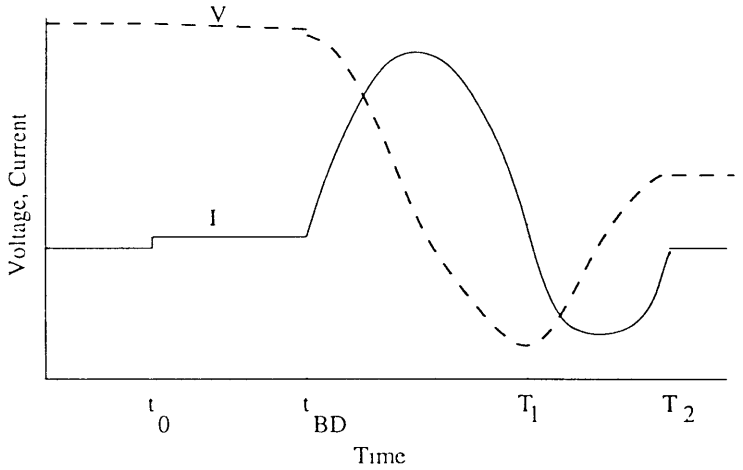

Figure 4-5: $i_L(t)$ and $V_C(t)$ vs. t

The switch is closed at time t_0. Since the spark gap does not immediately break

down, the capacitor discharges with an $RC = 33ms$ time constant. At time t_{BD} the gap breaks down and the capacitor discharges as in a characteristic RLC circuit through the gap. At time T_1, the arc in the spark gap extinguishes since there is no more current to maintain it. On a smaller time scale, the arc dies when it is cooled at a greater rate than the current can produce heat. This lack of current has the further effect of opening the switch. Beyond T_1, current flows back into the capacitor after the diode D1 begins to conduct. Current continues to flow through D1 as in an RLC circuit. At T_2, D1 stops conducting and all energy not used during the discharge has been restored in the capacitor.

Given that the specifications only apply to discharge, C and $L + L_{l1}$ are set to control $i_L(t)$ and ω in the discharge RLC circuit. Since the effective resistance through the diode D1 is less than the resistance through the switch, the coaxial cable, and the spark gap, the second RLC path is only slightly damped, and, therefore, more efficient.

4.2 Control Circuit

4.2.1 MCT

Component	Value
R1, R2, R8, R13, R14	open
JP1, JP2, JP3	closed
R12	10 MΩ
C5, C6	open
C7	0.01 μF

Table 4.3: HIP2030EVAL Components

Figure 4-6 provides the wiring diagram for an MCT-based control circuit. Table 4.3 gives appropriate settings of the HIP2030EVAL board. During a typical sequence, the control circuit receives a "fire" signal from the AUV. This signal is fed directly into a Schmitt trigger monostable vibrator (74LS221). The output pulse turns the HIP2030 to the "on" state. The width of the pulse needs to be just long enough to

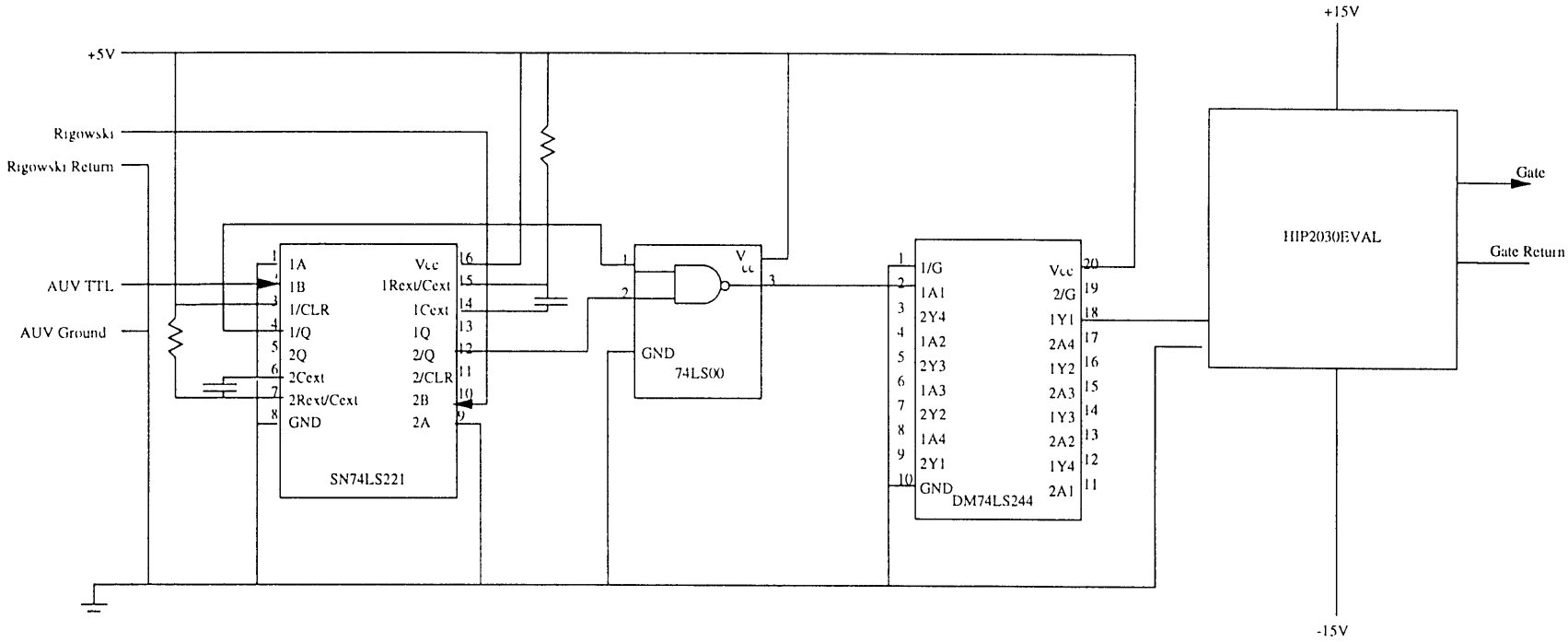

Figure 4-6: MCT Control Circuit Wiring Diagram

ensure breakdown.

When breakdown begins, a current pulse of peak 2,000A flows through the cabling. A Rigowski coil is put around one of these cables so as to register this current pulse. The voltage from this coil serves as input to another monostable vibrator. The output pulse width of this second monostable vibrator is set equal to the period of the discharge circuit. The outputs of the two monostable vibrators are processed (in the 74LS00), and the result directs the HIP2030 to turn the MCT "off" after one cycle of the discharge circuit. This is an optimal time to turn the MCT off for two reasons. First, the current through the MCT is zero, so the stress on the MCT is small. Second, the voltage on the capacitor is at a peak, so energy that was not dissipated during the discharge is conserved as much as possible.

The 74LS244 is a line driver able to source 64mA.

4.2.2 SCR

The wiring diagram of an SCR-based control circuit is shown in Figure 4-7. The 6N139 optically isolates the AUV electronics from the control circuit. The output of the 6N139 drives the monostable vibrator to output a pulse of width

$$ln(2)R_{ext}C_{ext} = ln(2)(22 \cdot 10^3)(0.001 \cdot 10^{-6}) = 15\mu s$$

This pulse width is longer than the turn-on time of the SCR, 1.5 μs. The 74LS244 line driver provides the necessary 50mA gate trigger current. Once this SCR is turned on, the 0.1 uF capacitor is discharged through the gate of the SCR's in the discharge circuit, triggering them.

4.3 Spark Gap

A drawing of the spark gap is shown in Figure 4-8. The anode and the cathode were 1/4"-20 screws in the tests, although the important dimension is 1/4 inch. A greater diameter will lead to excessive prebreakdown losses. A smaller diameter will

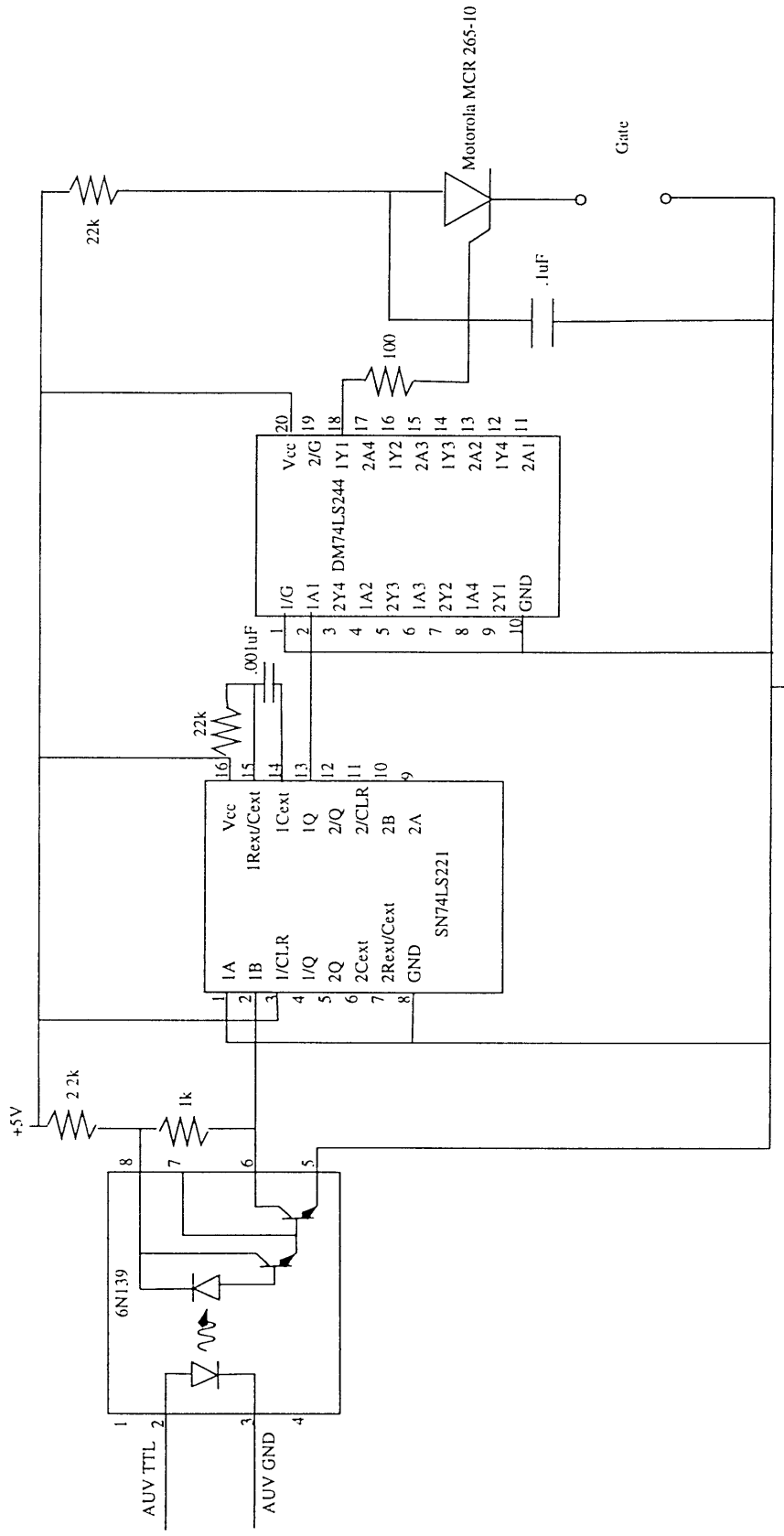

Figure 4-7: SCR Control Circuit Wiring Diagram

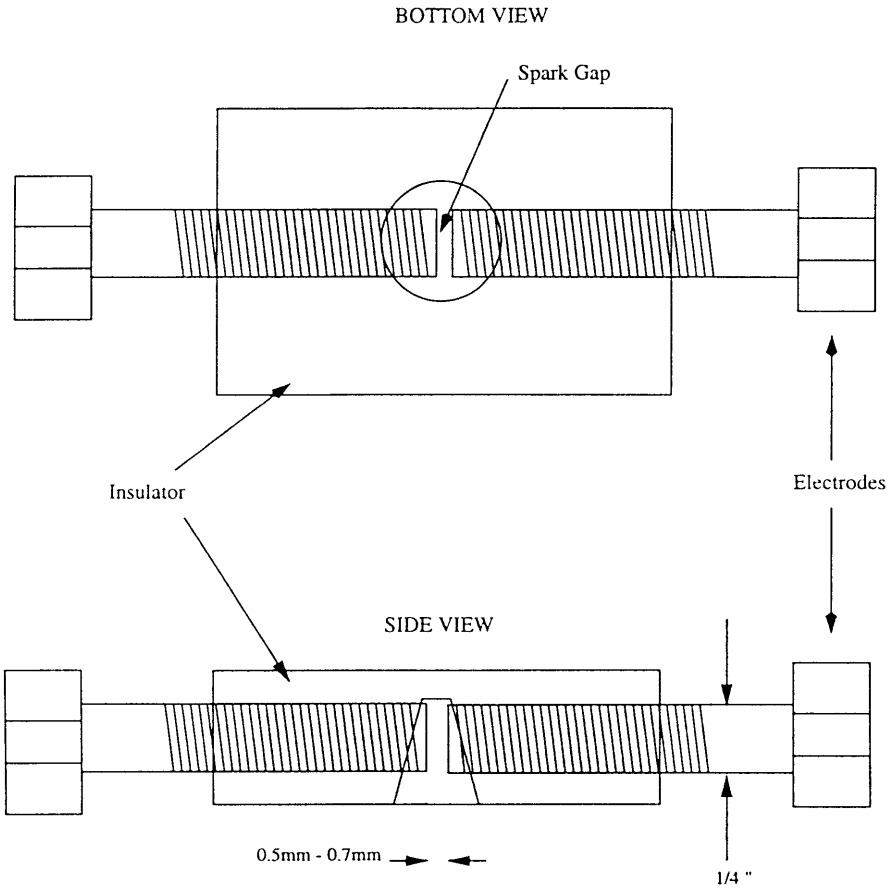

Figure 4-8: Spark Gap

decrease electrode lifetime. These electrodes were constructed of Grade 8 zinc-plated steel (extra hard). The gap length should be short, but long enough to not impede acoustic output. Lengths between 0.5mm and 0.7mm are appropriate.

4.4 Power Source

HVPS

A wiring diagram of the HVPS's is in Figure 4-9. The conversion efficiency of these devices is at best 85 %. The input ground, output ground, and signal ground are internally connected. Therefore, care must be taken to avoid ground loops.

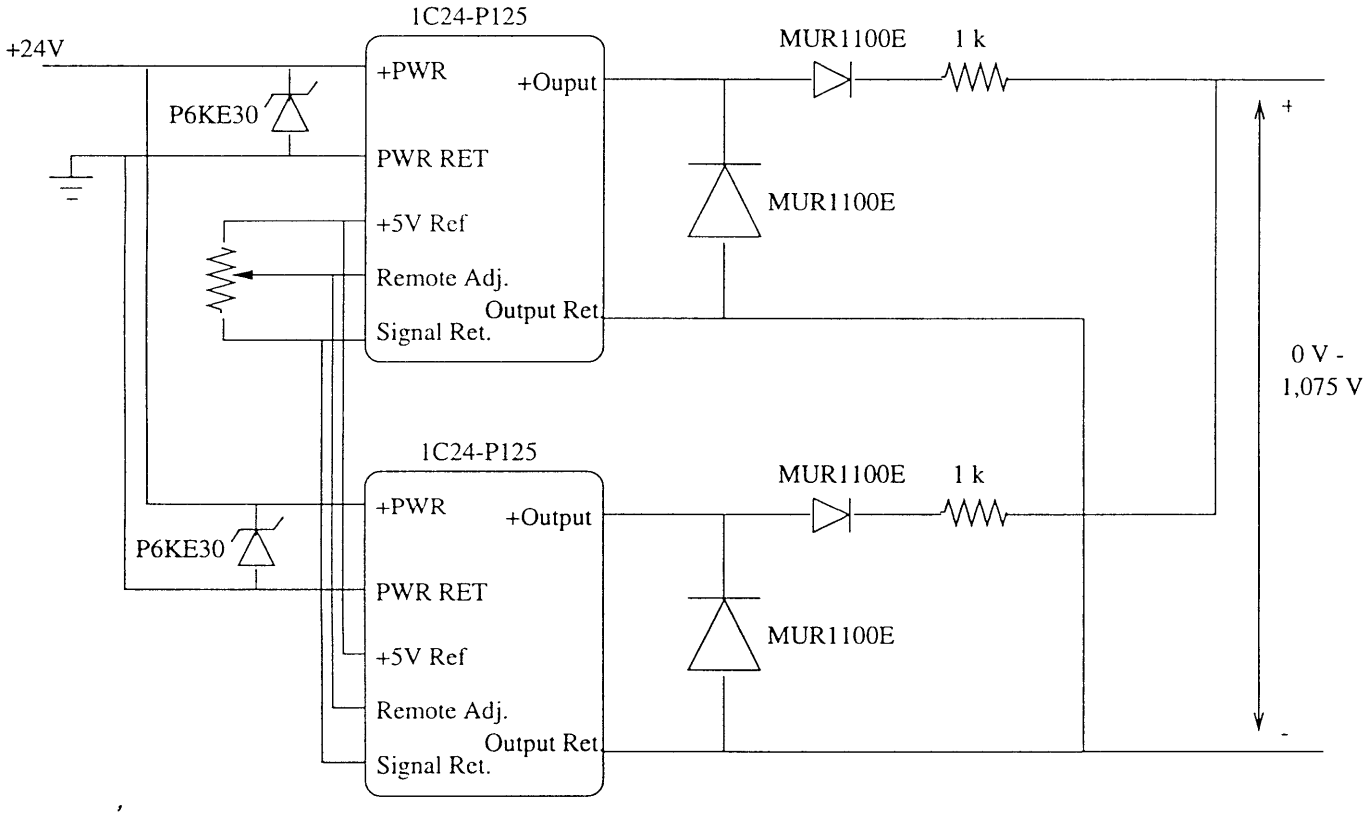

Figure 4-9: HVPS Wiring Diagram

The P6KE30 transient voltage suppressor protects the internal transistors from spurious voltages. These were added at the recommendation of James Morrison of Ul-

travolt, Inc. when a HVPS ceased operating without explanation. The MUR1100E's are fast (less than 1 μs) diodes that, together with the 1 kΩ resistors, protect the internal current-limiting circuitry during voltage swings on the output. The diodes in series with the 1 kΩ resistors are also needed for parallel combination of the HVPS's. The total resistance at the remote adjustment should be 30 kΩ. See Ultravolt Application Note 1.

Other Converters

The 1kV isolation DC-DC converters are supplied by International Power Sources, Inc. The +5V, 0V, -5V converter is an NMA2405S and the +15V, 0V, -15V converter is an NMA2415S. Both produce 1W.

Chapter 5

Conclusions

5.1 Characterization

The spark gap was fired in a plastic bucket filled with water from the Charles River. The operating voltage was 890V.

A typical current waveform appears in Figure 5-1. A corresponding waveform for the voltage across the spark gap is in Figure 5-2. Sampling these waveforms and multiplying gives the waveform for the power in Figure 5-3. Numerically integrating over time yields the total energy deposited in the spark gap, 21J. And the Fourier transform of this data yields the energy spectrum in Figure 5-4. The useful energy for sub-bottom profiling excludes frequencies greater than 10 kHz. The useful energy is, therefore, 19J.

The evolution of the spark gap over multiple firings can be analyzed in a similar manner. First, the evolution of energy, in time, can be seen in Figure 5-5. In the frequency domain, the evolution is as in Figure 5-6. Figure 5-7 displays the relative energy deviation of a discharge from the initial discharge.

The volume and mass of the USPG components are specified in Table 5.1.

Given this volume, the mass of water that will be displaced is 1.6 kg. Since the total mass of the system is 4.7 kg, the difference, 3.1 kg, is well below the 5 kg specification.

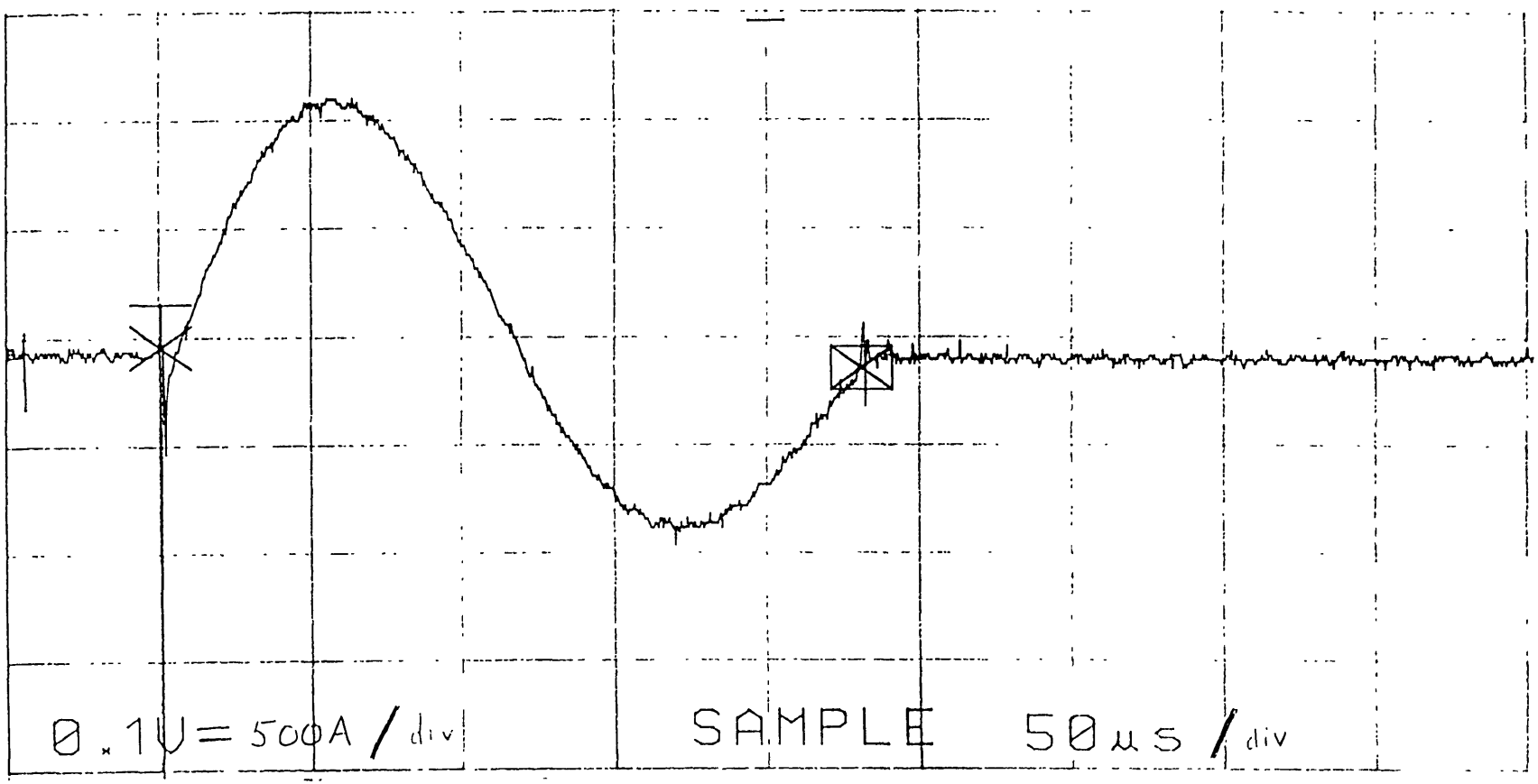

Figure 5-1: Sample Current Waveform

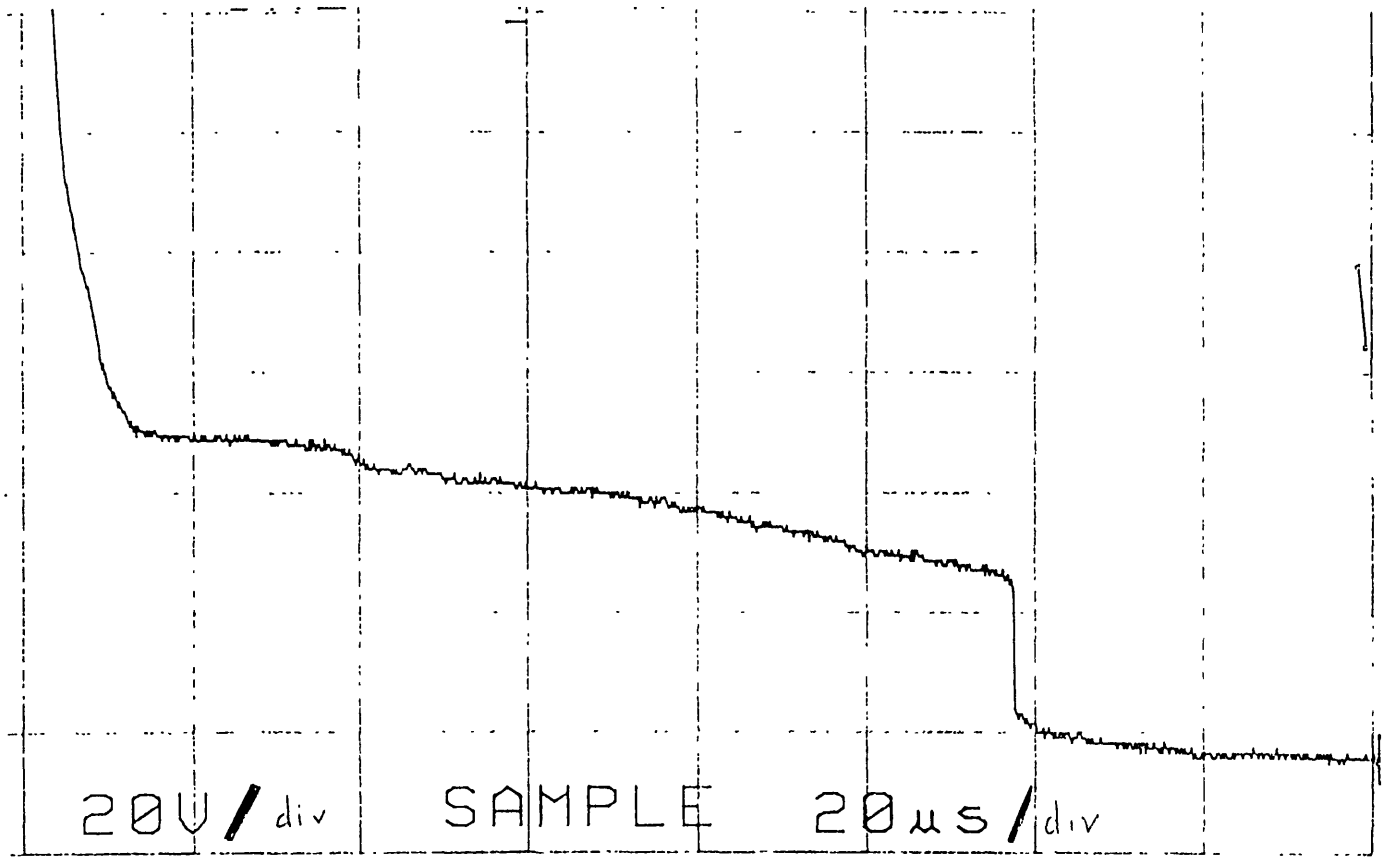

Figure 5-2: Sample Voltage Waveform

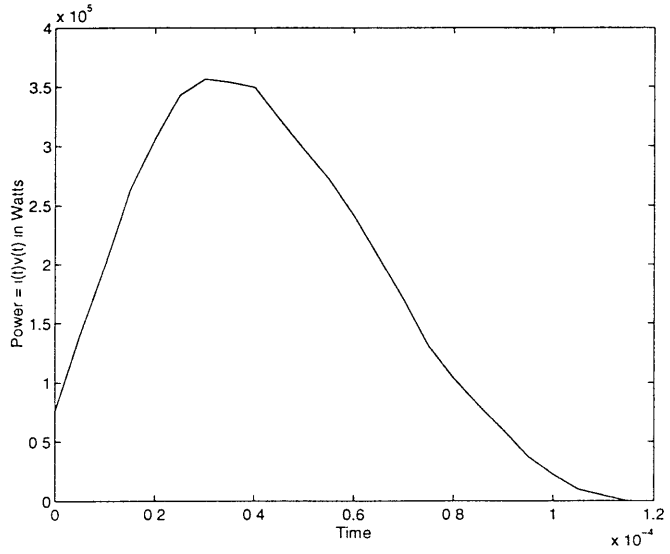

Figure 5-3: Power vs. t

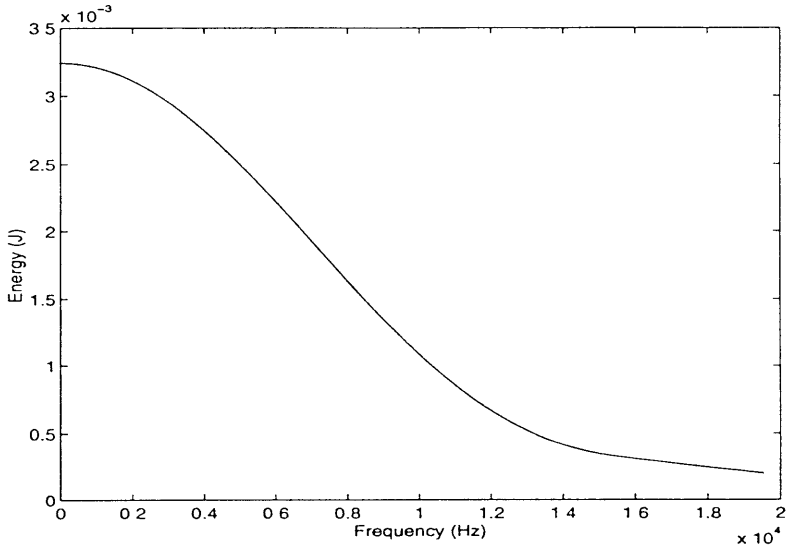

Figure 5-4: Energy Spectrum

Component	Volume (cm^3)	Mass (kg)
HVPS	300	2.64
Capacitor	1,250	1.64
Control Circuit	10	0.1
Inductor	50	0.4
Total	1,610	4.7

Table 5.1: Volume and Mass by Component

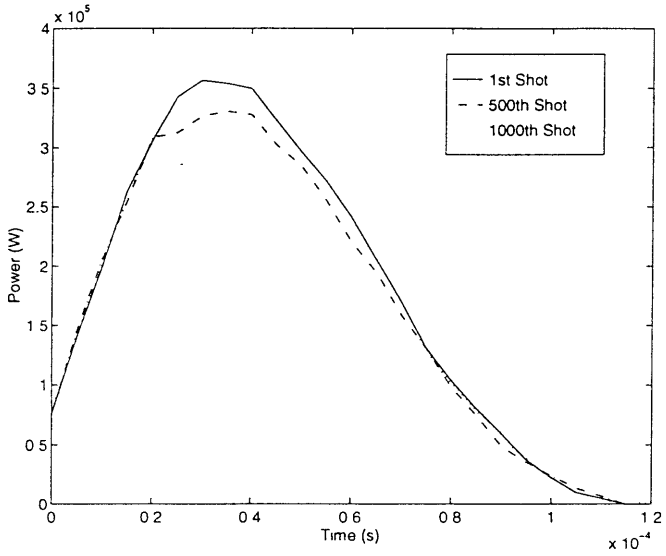

Figure 5-5: Evolution of Power

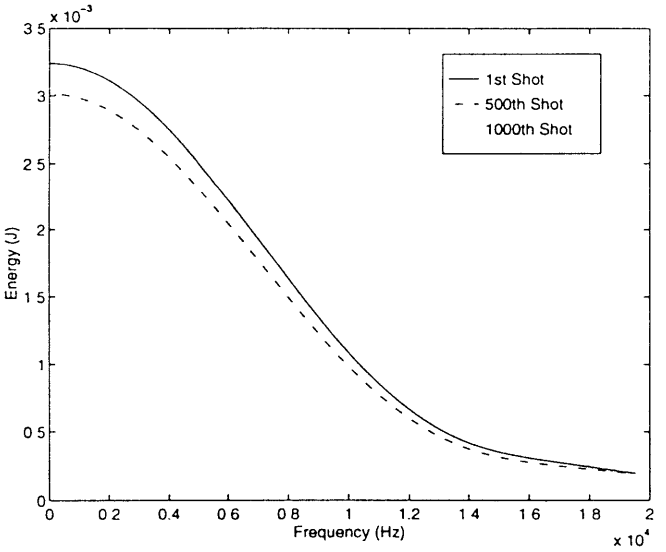

Figure 5-6: Evolution of Energy Spectrum

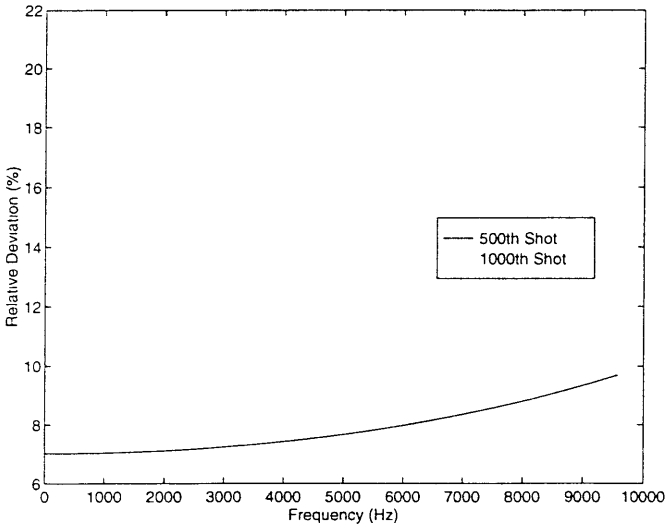

Figure 5-7: Relative Energy Deviation from 1st Discharge

5.2 Matching Specifications

A comparison of the product and the design specifications can be seen in Table 5.2. The final USPG is clearly applicable for operation in an AUV. The size and mass specifications, the most severe constraints, have been met with significant margins for expansion. The easiest expansions would be the addition of a third HVPS that would increase the repetition frequency to 5 Hz. The volume would still be appropriate for the specified cylinder.

The prototype lags expectations in terms of energy, lifetime, and reliability. These problems are being addressed by a new electrode design and the use of a more robust SCR that is capable of switching greater voltages. This increase in voltage will easily solve energy difficulties. However, the most serious concern is with reliability. Occasionally, the gap breaks down but the SCR does not open. The new SCR will hopefully overcome this problem. Another solution is to apply a negative bias to the gate. On other occasions, breakdown does not happen at all and the capacitor simply discharges. This may be caused by the deionization of the water in the vicinity of the electrodes. If that is the case, this problem will not be present in the field where water is continuously replaced.

Parameter	Specification	Product
Electrical Energy	20J	19J
Battery Volume	3,400cm^3	2,400cm^3 for recommended batteries
Electronics Volume	6,360 cm^3 in 18cm diameter, 25 cm length cylinder	1,610 cm^3. will fit in cylinder
Electrode Location	< 2m from electronics	2m range
Mass above displaced mass	<5kg	3.1 kg
Repetition Frequency	2 - 4 Hz	2.16 Hz (1 HVPS)
Energy Spectrum	< 10kHz	95% of Energy is < 10kHz
Lifetime	1,000 shots for 1 hour	Less than 22% deviation
Environment	fresh or salt water	Tested in Charles River, better performance as conductivity increases
Control	rising edge TTL	any rising edge (<18V)

Table 5.2: Specification and Product Comparison

Appendix A

Recommendations for High Pressure

There are two areas where the design may fail at high pressure. The components in the oil-compensated sphere may fail. The spark gap may cease to breakdown.

While the HVPS and capacitor selected were said to operate in oil, the manufacturers were unable to give any information about the effect of high pressure on these components. The pressure limit will be determined by the HVPS. These specific HVPS's have a significantly higher power density (both weight and volume) than any other devices I found. If the capacitor fails before the HVPS, a new one will have to be specially built that uses the oil in the pressure-compensated container as the dielectric. I recommend CSI Technologies in this event.

Research indicates that high pressure significantly impedes breakdown[8]. Supposedly, this effect is the result of decreased bubble formation at higher pressures. To overcome this obstacle, the operating voltage must be increased. Increasing the operating voltage, however, is not a simple matter. The value of 1kV was chosen because it is the upper limit of small lightweight devices. Increasing this voltage will require replacing most of the components in the USPG. And these components will require more volume and have a greater mass than the specifications currently allow.

First, the HVPS and the supporting electronics will need to be replaced. Ultravolt supplies higher voltage power supplies, so this should not be a difficulty.

The topology of the USPG discharge circuit does not need to be changed, but all of the components do. Any significant change in voltage will require that the diode and the switch be replaced with puck devices. Puck devices are large, heavy, and require a significant clamping force to make electrical contact. Thus, not only will the devices themselves increase the volume and the mass of the system, but the clamp will have a significant impact as well. A capacitor with a higher voltage rating will also be needed.

Furthermore, increasing the voltage while meeting the frequency spectrum will require a greater percent reversal on the capacitor. This will decrease the lifetime of the capacitor. Also, it may cause a second arc across the spark gap, depending on the turn-off time of the switch. And, the high voltage and current will more rapidly deteriorate the electrodes.

Thus, reliability at higher pressure will compromise volume, mass, lifetime, bubble oscillation, and repeatability.

Bibliography

[1] J. Bernardes and M. F. Rose. "Electrical Breakdown Characteristics of Sodium Chloride - Water Mixtures". *4th IEEE Pulsed Power Conference*, edited by T. H. Martin, M. F. Rose, IEEE Cat. No. 83 CH1908-3, pp. 308-311, 1983.

[2] David D. Caulfield. "Predicting Sonic Pulse Shapes of Underwater Spark Discharges". *Deep-Sea Research*, Vol. 9, pp. 339-348, 1962.

[3] James Dillon Cobine. *Gaseous Conductors: Theory and Applications.* Dover Publications, Inc., New York, 1958.

[4] Dobrin and Savit. *Introduction to Geophysical Prospecting.* McGraw-Hill, New York, pp. 115-141, 1988.

[5] Anthony Lyle Donaldson. "Electrode Erosion in High Current, High Energy Transient Arcs". 1990.

[6] J. R. Fricke and Charles Mazel. "Marine Sparker Applications for Environmental Seismic Surveys". Research proposal, 1994.

[7] Harris Semiconductor. *MCT, IGBT's, Diodes.* Harris Corporation, Application Notes, pp. 10-1 – 10-37, 1995.

[8] H. M. Jones and E. E. Kunhardt. "The Influence of Pressure and Conductivity on the Pulsed Breakdown of Water". *IEEE Transactions on Dielectrics and Electrical Insulation*, Vol. 1 No. 6, pp. 1016-1024, 1994.

[9] Yukihiro Kamase, Masami Shimizu, Tadashi Nagahama, and Akira Mizuno. "Erosion of Spark Gap of Square-Wave High-Voltage Source for Ozone Generation". *IEEE Transactions on Industry Applications*, Vol. 29, No. 4, July/August, 1993.

[10] John G. Kassakian, Martin Schlecht, and George Verghese. *Priciples of Power Electronics.* Addison-Wesley Publishing Company, Inc., Reading, MA, 1991.

[11] Warren Moon. "The Acoustical Transmission Response of an Ocean Bottom Sedimentary Layer". Thesis, 1966.

[12] Motorola, Inc. *Thyristor Device Data.* Motorola, Inc., Theory and Applications, pp. 1.1-1 – 1.6-9, 1995.

[13] Claudia Rodriguez. "An Electrical Sparker System as a Sound Source for Environmental Seismic Surveys". Research Proposal, 1995.

[14] Y. Toriyama and U. Shinohara. "Electric Breakdown Field Intensity of Water and Aqueous Solutions". *Phys. Rev.*, Vol. 51, p. 680, 1937.